

 Open access • Posted Content • DOI:10.1101/2020.03.17.995704

## Temporal context actively shapes EEG signatures of time perception

— [Source link](#) 

Atser Damsma, Nadine Schlichting, Hedderik van Rijn

**Institutions:** University of Groningen

**Published on:** 18 Mar 2020 - bioRxiv (Cold Spring Harbor Laboratory)

**Topics:** Time perception

Related papers:

- [The Effect of a Regular Auditory Context on Perceived Interval Duration.](#)
- [Timing Rhythms: Perceived Duration Increases with a Predictable Temporal Structure of Short Interval Fillers.](#)
- [Perception of time in articulated visual events](#)
- [Modality-specific temporal constraints for state-dependent interval timing.](#)
- [Alpha/beta power compresses time in sub-second temporal judgments](#)

Share this paper:    

View more about this paper here: <https://typeset.io/papers/temporal-context-actively-shapes-eeg-signatures-of-time-17xmuijq5h>

Running head: CONTEXT ACTIVELY SHAPES TIME PERCEPTION

## **Temporal context actively shapes EEG signatures of time perception**

Atser Damsma<sup>1\*</sup>, Nadine Schlichting<sup>1</sup>, Hedderik van Rijn<sup>1</sup>

<sup>1</sup>Department of Psychology, University of Groningen, Grote Kruisstraat 2/1, 9712 TS, Groningen, the  
Netherlands

\*Corresponding author: Atser Damsma ([a.damsma@rug.nl](mailto:a.damsma@rug.nl))

1 **Abstract**

2 Our subjective perception of time is optimized to temporal regularities in the environment. This is  
3 illustrated by the central tendency effect: when estimating a range of intervals, short intervals are  
4 overestimated whereas long intervals are underestimated to reduce the overall estimation error. Most  
5 models of interval timing ascribe this effect to the weighting of the current interval with previous  
6 memory traces *after* the interval has been perceived. Alternatively, the *perception* of the duration  
7 could already be flexibly tuned to its temporal context. We investigated this hypothesis using an  
8 interval reproduction task in which human participants (both sexes) reproduced a shorter and longer  
9 interval range. As expected, reproductions were biased towards the subjective mean of each presented  
10 range. EEG analyses showed that temporal context indeed affected neural dynamics during the  
11 perception phase. Specifically, longer previous durations decreased CNV and P2 amplitude and  
12 increased beta power. In addition, multivariate pattern analysis showed that it is possible to decode  
13 context from the transient EEG signal quickly after both onset and offset of the perception phase.  
14 Together, these results suggest that temporal context creates dynamic expectations which actively  
15 affect the *perception* of duration.

16 *Keywords:* time perception; context; Bayesian perception; EEG

17 **Significance Statement**

18 The subjective sense of duration does not arise in isolation, but is informed by previous experiences.  
19 This is demonstrated by abundant evidence showing that the production of duration estimates is  
20 biased towards previously experienced time intervals. However, it is yet unknown whether this  
21 temporal context actively affects perception or only asserts its influence in later, post-perceptual  
22 stages as proposed by most current formal models of this task. Using an interval reproduction task, we  
23 show that EEG signatures flexibly adapt to the temporal context during perceptual encoding.  
24 Furthermore, interval history can be decoded from the transient EEG signal even when the current  
25 duration was identical. Thus, our results demonstrate that context actively influences perception.

26 **Introduction**

27 The way humans experience time is not only driven by the current stimulus, but is also  
28 influenced by previous experiences. According to Bayesian observer models, humans integrate noisy  
29 sensory representations (the likelihood) with previously learned stimulus statistics (the prior  
30 distribution). This is illustrated by the temporal context or central tendency effect: when presented  
31 with a range of intervals, short intervals are overestimated and long intervals are underestimated  
32 (Jazayeri & Shadlen, 2010). Furthermore, the prior distribution has been shown to be dynamically  
33 updated, such that more recent intervals have a greater influence on the current estimate (Dyjas,  
34 Bausenhardt, & Ulrich, 2012; Taatgen & van Rijn, 2011; Wiener, Thompson, & Branch Coslett, 2014).  
35 Although there is abundant behavioral evidence for Bayesian integration in human time perception  
36 (Acerbi, Wolpert, & Vijayakumar, 2012; Cicchini, Arrighi, Cecchetti, Giusti, & Burr, 2012; Gu,  
37 Jurkowski, Lake, Malapani, & Meck, 2015; Hallez, Damsma, Rhodes, van Rijn, & Droit-Volet, 2019;  
38 Jazayeri & Shadlen, 2010; Maaß, Riemer, Wolbers, & van Rijn, 2019; Maaß, Schlichting, & van Rijn,  
39 2019; Roach, McGraw, Whitaker, & Heron, 2017; Schlichting et al., 2018; Shi, Church, & Meck,  
40 2013), its temporal locus and neural underpinnings are not yet understood.

41 Computational models of interval timing often (implicitly) assume that only after perception  
42 has completed, the noisy interval percept is weighted with previous memory traces representing the  
43 prior (e.g., Di Luca & Rhodes, 2016; Jazayeri & Shadlen, 2010; Taatgen & van Rijn, 2011).  
44 Alternatively, however, prior experience might actively affect perception, as evidenced by recent  
45 behavioral (Cicchini, Benedetto, & Burr, 2020; Cicchini, Mikellidou, & Burr, 2017; Zimmermann &  
46 Cicchini, 2020), fMRI (St. John-Saaltink, Kok, Lau, & De Lange, 2016) and single neuron findings  
47 (Sohn, Narain, Meirhaeghe, & Jazayeri, 2019). Specifically, Sohn et al. (2019) showed that neurons in  
48 the prefrontal cortex of monkeys exhibited different firing rate patterns based on the prior during  
49 interval estimation.

50 In humans, evidence is now emerging that electroencephalography (EEG) signatures in  
51 timing tasks are modulated by recently perceived durations. In a bisection task, longer prior durations  
52 led to a larger amplitude of the contingent negative variation (CNV) and increased beta oscillations  
53 power (Wiener, Parikh, Krakow, & Coslett, 2018; Wiener & Thompson, 2015). Crucially, however,

54 these studies required an active comparison to the standard interval, in which EEG signatures have  
55 been shown to reflect an adjustment of the decision threshold (Ng, Tobin, & Penney, 2011; see also  
56 Boehm, Van Maanen, Forstmann, & van Rijn, 2014). Any context-based changes in these signatures  
57 might reflect updating of the comparison process. It is therefore still an open question what the  
58 temporal locus of the context effect is: Does the prior exert its influence in post-perceptual stages or  
59 are purely perceptual processes already affected by previous experiences?

60 We tested the influence of temporal context in an interval reproduction task, which allowed us  
61 to distill EEG signals during the perception phase in which no decision or motor response was  
62 required that could yield fallacious conclusions regarding the effect of context effects during  
63 perception. Participants reproduced two different interval ranges (the *short* and the *long context*). The  
64 ranges shared one interval (the *overlapping interval*), providing a condition in which the physical  
65 stimulus was the same, but the temporal context was different. We show that temporal context affects  
66 three EEG signatures that have previously been associated with time perception during the perception  
67 phase: the CNV and beta oscillations, but also the offset P2, which has been shown to predict  
68 subjective interval perception better than the CNV (Kononowicz & van Rijn, 2014; Kruijne, Olivers,  
69 & van Rijn, 2021). A data-driven approach reveals that temporal context can be decoded from  
70 transient neural dynamics during the perception phase using multivariate pattern analysis (MVPA).  
71 Together, these results show that temporal context actively shapes the perception of duration,  
72 falsifying most current formal theories of interval timing.

## 73 **Materials and Methods**

### 74 **Participants**

75 Twenty-seven healthy adults (22 females; age range 18 - 33 years,  $M = 21.33$ ,  $SD = 3.78$   
76 years) participated in the experiment for course credits in the University of Groningen Psychology  
77 program or monetary compensation (€ 14). Two participants were excluded from analysis during pre-  
78 processing due to excessive artifacts in the EEG data. The study was approved by the Psychology  
79 Ethical Committee of the University of Groningen (17141-S-NE). Written informed consent was

80 obtained before the experiment. After the experiment, the participants were debriefed about the aim of  
81 the study.

## 82 **Stimuli and apparatus**

83 Stimuli were presented using the Psychophysics Toolbox 3.0.12 (Brainard, 1997; Kleiner et  
84 al., 2007) in Matlab 2014b. Intervals were presented as continuous 440 Hz sine wave tones. These  
85 auditory stimuli were presented on Sennheiser HD 280 Pro stereo headphones at a comfortable sound  
86 level. Visual stimuli were presented in the center of the screen in Helvetica size 25 in white on a dark  
87 grey background using a 27-inch Iiyama ProLite G27773HS monitor with a 1920x1080 resolution at  
88 100 Hz. The index-finger trigger buttons of a gamepad (SideWinder Plug & Play Game Pad,  
89 Microsoft Corporation) were used to record responses.

## 90 **Procedure**

91 Participants performed an auditory interval reproduction task (Figure 1A). Every trial started  
92 with a central fixation cross with a uniform random duration between 2 and 3 s. Then, an exclamation  
93 mark was presented for 0.7 s, after which the auditory interval was presented (the *perception phase*)  
94 while the exclamation mark remained on the screen. To signal the next phase, the exclamation mark  
95 was replaced by a question mark which was presented for 1.5 s. Next, the continuous tone was  
96 presented again, with the question mark remaining on the screen, which participants had to terminate  
97 by pressing a button (the *reproduction phase*). Participants were instructed to match the duration of  
98 this second tone to the duration of the first tone as accurately as possible.

99 The task involved two different interval ranges, the short context (0.625 s, 0.75 s, and 0.9 s)  
100 and the long context (0.9 s, 1.08 s, and 1.296 s) (Figure 1A). Crucially, there was an *overlapping*  
101 *interval* that was presented in both contexts (0.9 s). The experiment consisted of four blocks, two of  
102 which used intervals of the short context, and two of which used intervals of the long context. Block  
103 order was counterbalanced across participants, with the constraint that the context would alternate  
104 every block. Within a block, each duration of the short or the long context was presented 30 times,  
105 amounting to a total of 90 trials per block and 360 trials over the whole experiment. The presentation  
106 order was random, with the constraint that every possible subsequent pair of intervals was presented  
107 equally often (i.e., first-order counterbalancing). The hand needed for reproduction was switched after

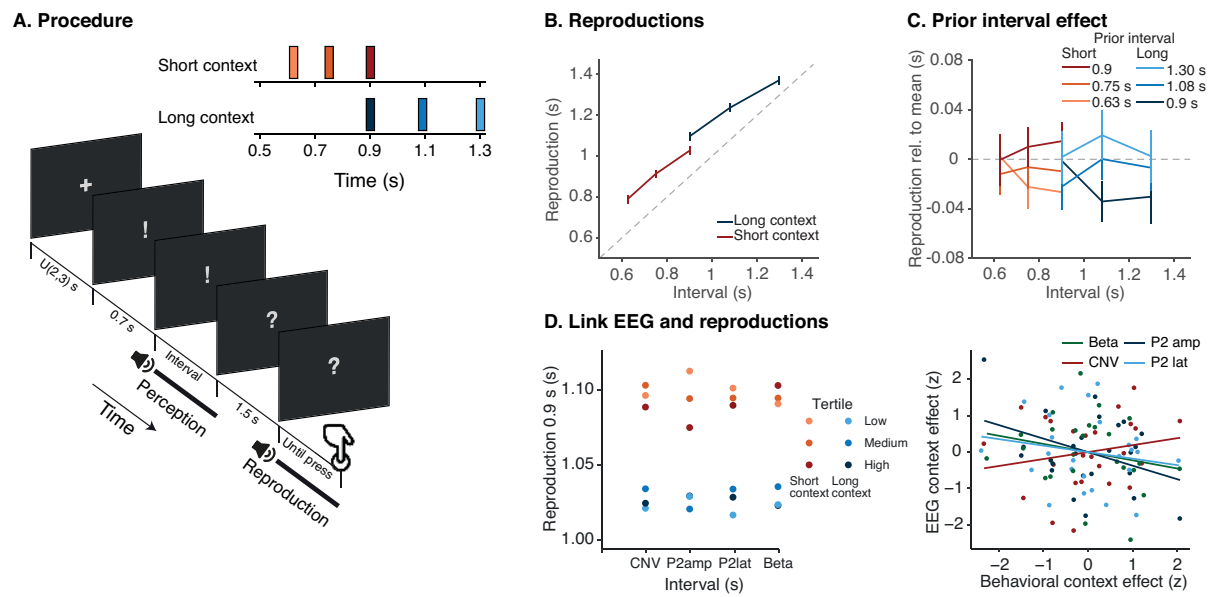


**Figure 1.** Task and behavioral results. A) Behavioral procedure of the experiment. Participants performed an interval reproduction task in which they heard a tone for a certain duration (*perception phase*). After an ISI of 1.5 s, they were asked to reproduce this duration by pressing a button to indicate the offset of the *reproduction phase*. In separate blocks, the perception phase consisted of three short or three relatively long durations (the *short* and the *long context*, respectively). One interval was presented in both contexts (the *overlapping interval* of 0.9 s). B) Average behavioral reproduction results. Error bars represent the standard error of the mean. C) Average reproduction of the overlapping interval (0.9 s) for the different intervals in the previous trial, relative to average reproduction in the context condition. Overall, reproductions were longer when the prior interval was longer. D) Link between the EEG signatures and reproductions. The left panel shows the reproduction of the overlapping interval for relatively low, medium, and high values (i.e., tertiles) of the CNV amplitude, P2 amplitude, P2 latency, and beta power. The right panel shows the correlation between participants' behavioral context effect and their context effect in the different EEG signatures (all values were z-scored). Dots represent individual participants, while the lines represent linear regression lines.

108 two blocks. Prior to each block, participants were instructed which hand (i.e., which gamepad button)

109 they would use to terminate the duration and which set of intervals would be presented (termed set A

110 and set B for the short and long context, respectively; see also Maaß, Schlichting, et al., 2019), while

111 they were not informed about the relative durations or distributions associated with the sets (i.e., that

112 the sets were associated with a short and long interval range). Participants could take self-timed

113 breaks between blocks. Prior to the experiment, participants performed two practice trials with

114 durations outside the range of both context conditions (0.4 s and 2 s). Experiment scripts are available

115 at <https://osf.io/sgbjz/>.

## 116 EEG acquisition

117 EEG signals were recorded from 62 Ag/AgCl electrodes, placed in accordance with the

118 international 10-20 system (WaveGuard EEG cap, eemagine Medical Imaging Solutions GmbH,

119 Berlin, Germany). The ground electrode was placed onto the left side of the collarbone and the  
120 mastoids served as location for the reference electrodes. The electrooculogram (EOG) was recorded  
121 from the outer sides of both eyes and from the top and bottom of the left eye. Data was collected at a  
122 sampling frequency of 512 Hz using a TMSi Refa 8-64 amplifier. Before the experiment, impedances  
123 of all electrodes were reduced to below 5k $\Omega$ . Participants were instructed to blink only between trials  
124 and not to move during the experiment.

### 125 **EEG pre-processing**

126 EEG pre-processing was performed using the FieldTrip toolbox (Oostenveld, Fries, Maris, &  
127 Schoffelen, 2011). EEG data was re-referenced to the averaged mastoids and filtered using a  
128 Butterworth IIR band-pass filter with a high-pass frequency of 0.01 Hz and a low-pass frequency of  
129 80 Hz. Subsequently, trial epochs were created from -1 s until 6 s relative to the onset of the  
130 perception phase. Artifacts were corrected using independent component analysis (ICA). Epochs that  
131 exceeded an amplitude range of 120  $\mu$ V were removed from the dataset. On average, 10.72% ( $SD =$   
132 6.10) of the 360 trials were discarded.

### 133 **Data Analysis**

134 **Behavioral analysis.** Reproductions lower than 0.1 s and higher than 2 s were excluded from  
135 analysis (0.2% of the data). To test whether reproductions were influenced by context, we fitted a  
136 linear mixed model (LMM) using the *lme4* package (Bates, Mächler, Bolker, & Walker, 2015) in R  
137 (R Core Team, 2016), including interval, context, their interaction and prior interval (i.e., the interval  
138 in the previous trial) as fixed factors. To facilitate interpretation of the results, interval and prior  
139 interval were centered at 0.9 s and the factor context was recoded using effect coding (-0.5 for short  
140 and 0.5 for long context). In addition to the random intercept of participant, we sequentially added  
141 random slope terms and tested whether they improved the model with a likelihood ratio test. We will  
142 here report the results of the best fitting model, which included random slopes for interval and prior  
143 interval.

144 **ERP analysis.** All EEG analyses reported here focused on the perception phase. An overview  
145 of the EEG results in the reproduction phase is available in the supplementary materials (section 1) at



146 <https://osf.io/sgbjz/>. The CNV and beta signatures in the reproduction phase show trends that are  
147 qualitatively similar to the perception phase, although they appear to be less strong.

148 **CNV.** The CNV analysis was performed on a fronto-central electrode cluster (electrodes Cz,  
149 C1, C2, FCz, FC1, FC2) (Kononowicz & van Rijn, 2014; Ng et al., 2011). A 10 Hz Butterworth low-  
150 pass filter was applied and the ERP was baselined to the average signal in the 0.1 s window before  
151 interval onset. To test the effect of global context during the perception phase, we compared the ERP  
152 of the overlapping interval in the short and the long context using a cluster-based permutation test  
153 (Maris & Oostenveld, 2007) in the window 0-1.2 s from interval onset. The permutation test assessed  
154 whether the difference was different from zero by computing 100.000 permutations using the *t*-  
155 statistic, controlling for multiple comparisons with a cluster significance threshold of  $p < .05$ . To  
156 assess the influence of the prior interval on CNV, we calculated the average amplitude in the time  
157 window that showed CNV differences in the previously mentioned permutation test (0.3-1.01 s), per  
158 participant, context and prior interval for the overlapping interval. Next, we tested an LMM predicting  
159 this amplitude, including context and prior interval as fixed factors, and participant as a random  
160 intercept term.

161 **Offset P2.** The P2 analysis focused on the EEG signal averaged over the same fronto-central  
162 electrode cluster as the CNV analysis, to which a 1–20 Hz Butterworth band-pass filter was applied to  
163 minimize CNV-based contamination (cf., Kononowicz & van Rijn, 2014). The ERP was baselined to  
164 the average signal in the 0.1 s window around interval offset (cf., Kononowicz & van Rijn, 2014).  
165 Similar to the CNV analysis, the ERPs of the overlapping interval in the short and the long context  
166 were compared using a cluster-based permutation test in the window 0-0.5 s after interval offset.  
167 Next, we calculated P2 amplitude was as the average amplitude between 0.14 and 0.3 s after interval  
168 offset (this window was based on Kononowicz & van Rijn, 2014). We fitted an LMM predicting P2  
169 amplitude, with interval, prior interval, and context as fixed factors, and participant as a random  
170 intercept term. The random slope of interval improved the fit and was added to the model. P2 latency  
171 was calculated as the 50% area latency - the time point at which half of the area under the curve is  
172 reached - within the same window (Liesefeld, 2018; Luck, 2005). P2 latency was analyzed using an  
173 LMM with the same fixed factors as the P2 amplitude model.

174           Because the 1 Hz high-pass filter might induce artifactual effects of opposite polarity before  
175 the actual peak (Tanner, Morgan-Short, & Luck, 2015), we also performed the P2 analysis on the data  
176 without additional filtering (that is, besides the band-pass filter between 0.01 Hz and 80 Hz applied  
177 during pre-processing). We found similar qualitative results, which are reported in the supplementary  
178 materials section 2.1 at <https://osf.io/sgbjz/>.

179           **Multivariate pattern analysis.** To investigate transient neural dynamics in more detail, we  
180 tested whether it is possible to decode global and local context through MVPA of the EEG signal.  
181 Following Wolff, Kandemir, Stokes, and Akyürek (2020), we used a sliding window approach in  
182 which the EEG fluctuations were pooled over electrodes and time. A window of 50 data points (98  
183 ms) was moved across the signal in steps of 8 ms, separately for each channel. Within the window, the  
184 signal was down-sampled to 10 samples (by taking the average over 5 samples) and baseline-  
185 corrected by subtracting the mean within the window from all 10 individual samples.

186           To decode whether an overlapping-interval trial was presented in the short or the long  
187 context, the 10 samples per electrode in each time window served as input for 5-fold cross-validation.  
188 In each fold, we calculated the Mahalanobis distance (De Maesschalck, Jouan-Rimbaud, & Massart,  
189 2000; Wolff, Jochim, Akyürek, & Stokes, 2017; Wolff et al., 2020) between the test trials and the  
190 averaged signal of the short and long context, using the covariance matrix estimated from the training  
191 trials with a shrinkage estimator (Ledoit & Wolf, 2004). To make the distance estimates more reliable,  
192 the 5-fold cross-validation was repeated 50 times and results were averaged. The eventual decoding  
193 distances were smoothed with a Gaussian smoothing kernel ( $SD = 16$  ms). To test whether the  
194 distance between conditions was significantly different from zero, a cluster-based permutation test  
195 was performed.

196           A similar analysis was performed to decode the duration of the prior interval from the neural  
197 dynamics in the current trial. For the overlapping interval, the Mahalanobis distance between every  
198 test trial and the average of the prior interval conditions was calculated. This resulted in six difference  
199 time series for each condition (including the 0.9 s condition for each context separately and the  
200 difference with the trial's own condition). In this way, we aimed to determine whether the distance  
201 was higher when the difference between the prior interval condition of the test trial and the other

202 possible prior interval conditions was larger. Next, for every time point, we performed a linear  
203 regression on the Mahalanobis distance, using the absolute difference between prior interval  
204 conditions (in seconds) and the difference between context (coded as 0 or 1) as predictors, allowing us  
205 to disentangle the effect of sequential and global context on transient neural dynamics. A cluster-  
206 based permutation test was performed on the resulting slope values for prior interval and context, to  
207 test whether they deviated from zero (using a one-sided *t*-test).

208 To investigate which electrodes are most informative in decoding the context of an  
209 overlapping interval trial, we performed channel-wise decoding: the procedure to decode global  
210 context outlined above was performed separately for every electrode. Topographies were created to  
211 show the average decoding accuracy at the different electrodes during time windows in which the  
212 Mahalanobis distance resulting from the context decoding procedure outlined above (i.e., using all  
213 electrodes) was significantly higher than zero.

214 Because the context conditions were blocked in our experimental design, the decoding  
215 accuracy might have been inflated by nonstationarities in the EEG signals, which lead to stochastic  
216 dependence between trials (Lemm, Blankertz, Dickhaus, & Müller, 2011). Post-hoc, we controlled for  
217 this notion by calculating the Mahalanobis distance between the different blocks, for each participant.  
218 This allowed us to differentiate between the distances between blocks that were presented in the first  
219 and second half of the experiment, and thereby, to test whether the original decoding results could be  
220 due to within-block similarities beyond context. In this way, we compared the Mahalanobis distance  
221 between the trials in a particular block and the ‘same context’ and ‘different context’ block in the  
222 other half of the experiment. We found that the results were qualitatively similar to the original  
223 analysis, with significant differences between the short and long context immediately after interval  
224 onset and after interval offset (analysis details and full results can be found in the supplementary  
225 materials section 2.2. at <https://osf.io/sgbjz/>).

226 **Time-frequency analysis.** To assess oscillatory power during the perception phase we  
227 performed a time-frequency analysis using a single Hanning taper with an adaptive time window of 6  
228 cycles per frequency in steps of 15 ms for frequencies from 4 to 40 Hz, with the amount of spectral  
229 smoothing set to 1. We calculated the absolute power from the baseline window of -0.2-0 s relative to

230 interval onset. The analysis was again focused on fronto-central electrodes (Cz, C1, C2, FCz, FC1,  
231 FC2). Similar to the CNV analysis, all time-frequency analyses were performed on the overlapping  
232 interval to isolate the effect of context while keeping the actual stimulus constant.

233 Per participant, for every time-frequency point, we fitted a linear regression model including  
234 prior interval (a continuous variable ranging from the shortest to the longest interval in seconds) and  
235 context (short and long context coded as 0 and 1, respectively) as predictors (following an approach  
236 similar to Wiener et al., 2018). For every time-frequency point, this resulted in two slope values,  
237 expressing the relative influence of the global context and the previous interval. Next, a one-sample *t*-  
238 test against zero was performed for the two slope values at each time-frequency point, which was  
239 corrected for multiple comparisons using cluster-based permutation (Maris & Oostenveld, 2007). The  
240 statistical testing was performed on the frequency range of 8-30 Hz to include alpha power (8–14 Hz;  
241 Kononowicz & van Rijn, 2015) and beta power (15–30 Hz; e.g., Haegens et al., 2011; Jenkinson &  
242 Brown, 2011; Kononowicz & van Rijn, 2015) during the time window of 0-1.2 s after interval onset.

243 **Linking EEG signatures and behavior.** We tested in two ways whether EEG signatures  
244 during the perception phase predicted behavioral reproductions. First, we computed *single trial* values  
245 of CNV amplitude, P2 amplitude, P2 latency and beta power. Following the methods described above,  
246 for every trial, CNV amplitude was calculated as the average EEG signal in the window 0.3-1.01 s  
247 after interval onset, P2 amplitude as the average between 0.14 and 0.3 s after interval offset, P2  
248 latency as the 50% area latency in the same window, and beta power was calculated as the average  
249 power in the time window 0.48-0.84 s after interval onset and the frequency range 23-30 Hz, which  
250 was based on the permutation test. CNV, P2 amplitude, P2 latency, and beta power values that  
251 deviated more than 4 SD from the average were excluded from analysis (0.06%, 0.01%, 0.00% and  
252 0.46% of the trials, respectively). Similar to the behavioral analysis described above, reproductions  
253 shorter than 0.1 s and longer than 2 s were also excluded from analysis. Next, we computed four  
254 LMMs with reproduction as the dependent factor, and CNV amplitude, P2 amplitude, P2 latency, and  
255 beta power as fixed factors, respectively. Similar to the analyses described above, the CNV and beta  
256 power analyses were focused on the overlapping interval trials. To control for the effect of context on  
257 both EEG signatures and behavior, context and prior interval were also added as fixed factors to the

258 models. The P2 analysis included all intervals, so here, interval was entered as an additional fixed  
259 factor. In all models, participant was included as a random intercept term, and adding random slopes  
260 did not improve the model fit in any of the models.

261 Second, in addition to the single trial analysis, we looked at individual differences: Do  
262 participants who show a large context effect in the EEG signatures also show a large behavioral  
263 context effect? To this end, for the overlapping interval, we estimated the behavioral context effect  
264 (i.e., the difference in reproduction between the long and short context) for each participant, and  
265 compared it to the context effect of CNV amplitude, P2 amplitude and latency, and beta power,  
266 quantified as described in the previous paragraphs. To assess whether these measures were related for  
267 each participant, we performed a one-tailed Pearson's correlation test between the individual  
268 behavioral context effects and the EEG context effects.

## 269 **Results**

### 270 **Behavioral results**

271 Figure 1B shows the average reproductions for the different intervals. The results of the LMM  
272 showed that the reproductions increased with duration ( $\beta = 0.77$ ,  $SE = 0.03$ ,  $t = 24.33$ ,  $p < .001$ ). We  
273 found a significant effect of global context, showing that reproductions were longer in the long  
274 compared to the short context ( $\beta = 0.05$ ,  $SE = 0.01$ ,  $t = 7.23$ ,  $p < .001$ ). In addition, the increase with  
275 duration (i.e., the slope) was lower for the long compared to the short context ( $\beta = -0.18$ ,  $SE = 0.03$ ,  $t$   
276  $= -7.01$ ,  $p < .001$ ). Besides the global context effect, reproductions were longer when the interval in  
277 the previous trial was longer ( $\beta = 0.08$ ,  $SE = 0.02$ ,  $t = 3.41$ ,  $p = .002$ ). Figure 1C shows the  
278 reproductions for the different previous intervals, relative to the average reproduction.

### 279 **ERPs**

280 **CNV.** Figure 2A and 2B show the average fronto-central ERP during the perception phase for  
281 the different intervals in the short and the long context, respectively. In addition, Figure 2D shows a  
282 direct comparison between the short and the long context of this ERP for the overlapping interval (0.9  
283 s). The cluster-based permutation test showed that the CNV was more negative in the short than in the  
284 long context in the time windows 0.30-0.65 s ( $p = .004$ ) and 0.71-1.01 s ( $p = .003$ ). Thus, while the

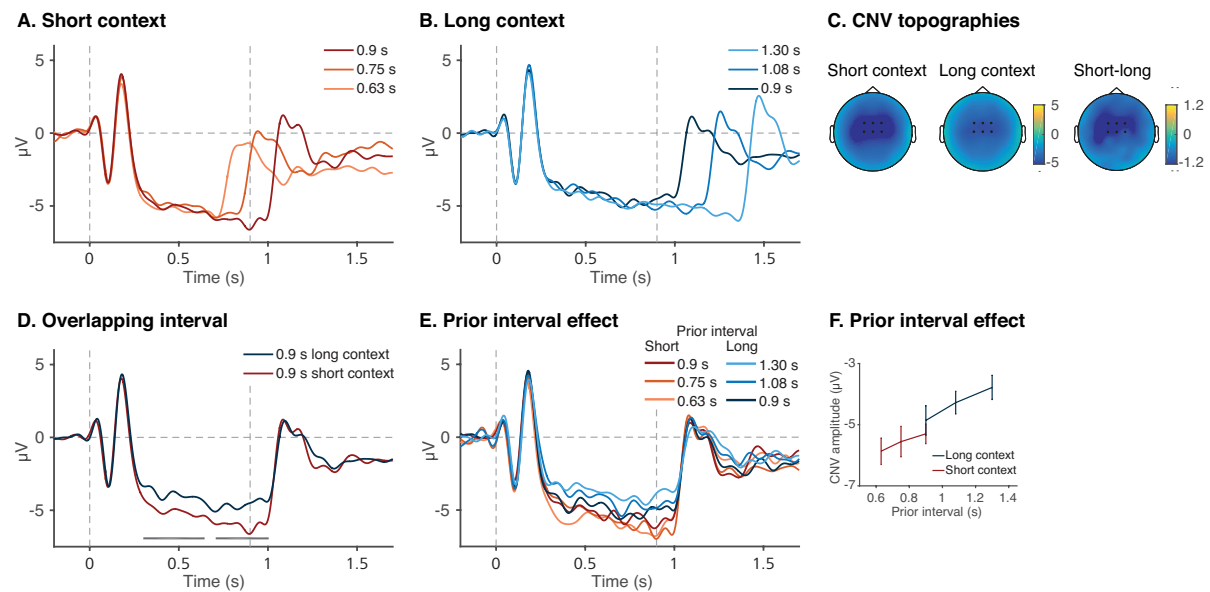


**Figure 2.** Average ERPs at the fronto-central cluster (Cz, C1, C2, FCz, FC1, FC2) relative to the onset of the perception phase for the different durations in the short (A) and long (B) context. In all panels, vertical grey dashed lines indicate interval onset and offset of the overlapping interval (0.9 s). C) Topographies of the overlapping interval (0.9 s), for the short context, long context, and their difference, during the window of significant difference as indicated by the cluster-based permutation test. D) Average ERP of the overlapping interval (0.9 s) in the short and the long context. Grey horizontal bars indicate significant differences according to the cluster-based permutation test. E) Average ERP of the overlapping interval, split up according to the interval in the previous trial. Red and blue lines show whether the overlapping interval appeared in the short or the long context, respectively. F) Average CNV amplitude for the middle interval, in the time window of significant difference between the short and long context, for the different previous intervals. Error bars represent the standard error of the mean.

285 actual interval was the same, CNV amplitude during perception differed depending on the temporal  
 286 context.

287 Figure 2E shows the average ERP for the overlapping interval, split for the different previous  
 288 durations, and Figure 2F shows the average CNV in the 0.3-1.01 s window for the different prior  
 289 interval conditions. The LMM results showed that CNV amplitude at the overlapping interval became  
 290 less negative with longer previous trials ( $\beta = 2.50$ ,  $SE = 0.97$ ,  $t = 2.57$ ,  $p = .011$ ). There was no  
 291 evidence for an additional significant effect of context ( $\beta = 0.43$ ,  $SE = 0.42$ ,  $t = 1.03$ ,  $p = .308$ ),  
 292 suggesting that the global context effect on CNV might be largely driven by the previous trial. Post-  
 293 hoc, we tested whether including the interaction between context and prior interval improved the  
 294 model fit, but a likelihood ratio test showed that this was not the case ( $\chi^2(1) = 0.10$ ,  $p = .750$ ).

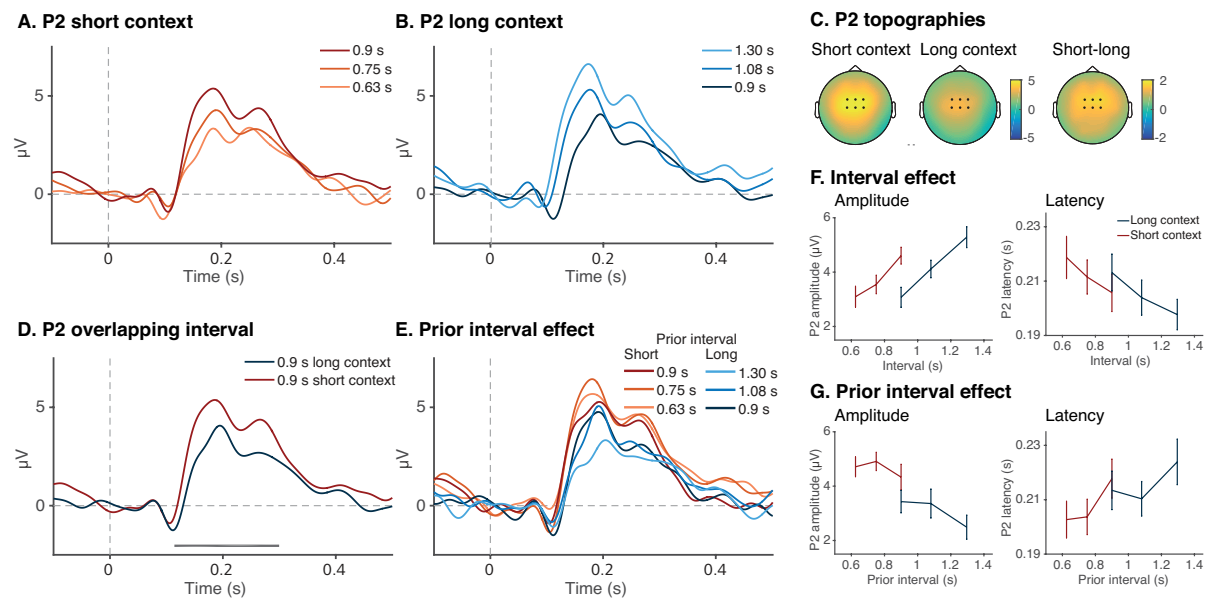


**Figure 3.** Amplitude and latency of the P2 at the fronto-central cluster (Cz, C1, C2, FCz, FC1, FC2) after the offset of the perception phase. A, B) Grand average ERPs baselined at the offset of the perception phase in the short and the long context, respectively. C) Topographies of P2 amplitude of the overlapping interval (0.9 s), for the short context, long context, and their difference, during the window of significant difference as indicated by the cluster-based permutation test. D) Average ERP of the overlapping interval (0.9 s) in the short and the long context. Grey horizontal bars indicate significant differences according to the cluster-based permutation test. F) Effect of interval on P2 amplitude and latency. The left panel shows P2 amplitude, calculated as the average amplitude in the window 0.14-0.3 s after interval offset for every participant and interval. The right panel shows P2 latency, calculated as the 50% area latency in the same window. G) Effect of the prior interval on P2 amplitude (left) and latency (right). In all figures, error bars represent the standard error of the mean.

295 **Offset P2. Amplitude.** Figure 3A and 3B shows the offset P2 for the different intervals in the  
 296 short and the long context, respectively. Figure 3D directly compares the P2 for the overlapping  
 297 interval in the short and long context. The cluster-based permutation test showed that the amplitude  
 298 was higher for the short compared to the long context in the window 0.11-0.3 s. Figure 3F shows the  
 299 average P2 amplitude as a function of interval and context. The LMM showed that the P2 increased  
 300 with duration ( $\beta = 5.56, SE = 0.62, t = 8.97, p < .001$ ), but that the intercept was significantly lower  
 301 for the long compared to the short context ( $\beta = -0.87, SE = 0.28, t = -3.10, p = .002$ ). Figure 3E and  
 302 3G (left panel) show the effect of the prior interval on P2 amplitude for the overlapping interval. In  
 303 line with the global context effect, the model showed that the P2 decreased with longer previous  
 304 intervals ( $\beta = -1.71, SE = 0.51, t = -3.35, p = .001$ ). Together, these results show that P2 amplitude  
 305 reflects the actual duration, as well as the global and local context in which the duration appeared.

306 **Latency.** Figure 3F (right panel) shows that P2 latency decreased with the duration of the  
307 current interval, which was confirmed by the LMM predicting latency ( $\beta = -0.04$ ,  $SE = 0.01$ ,  $t = -3.66$ ,  
308  $p < .001$ ). There was no evidence that P2 latency was affected by the context, as the fixed factors  
309 context and prior interval did not reach significance ( $ps > .247$ ). In summary, whereas P2 amplitude  
310 reflects the current duration and the general and sequential temporal context, P2 latency only  
311 decreases with longer current durations.

### 312 **Multivariate pattern analysis**

313 Figure 4A shows the decoding accuracy for the overlapping interval. The permutation test  
314 showed a positive cluster immediately after interval onset (0-0.17 s;  $p = .009$ ) and after interval offset  
315 (0.99-1.37 s;  $p < .001$ ). Figure 4C shows the topographies of the channel-wise decoding results during  
316 these two clusters, which reflects high parietal and left-lateralized decoding accuracy and high fronto-  
317 central and right-lateralized decoding accuracy, respectively. Figure 4B shows the slope value of prior  
318 interval in the regression analysis predicting Mahalanobis distance. The permutation test showed that  
319 there was no evidence for significant clusters for the slope of prior interval or context in the regression  
320 analysis ( $p = .999$ ), showing that MVPA could not distinguish between prior interval conditions based  
321 on the transient EEG signal.

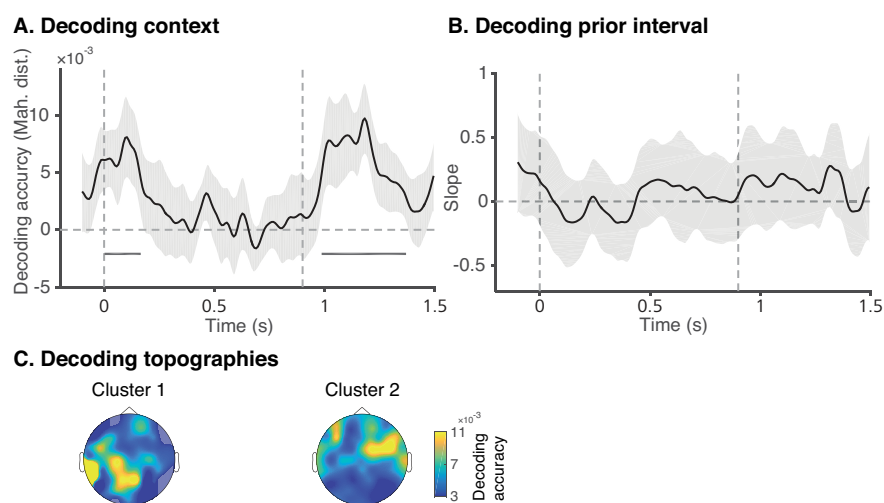


**Figure 4.** Decoding accuracy relative to the onset of the perception phase. A) Decoding accuracy of context for the overlapping interval as represented by the Mahalanobis distance. Grey horizontal bars indicate a significant difference from zero according to the cluster-based permutation test. Error shading represent 95% CI of the mean. B) Decoding accuracy of prior interval in the overlapping interval, represented by the slope value of the regression of Mahalanobis distance with prior interval and context as predictors. C) Topographies of channel-wise context decoding accuracy for the overlapping interval, during the first significant cluster in panel A (left) and the second cluster (right). Colors represent the decoding accuracy in Mahalanobis distance.



322 **Time-frequency analysis**

323 To assess oscillatory power during the perception phase, we calculated a linear regression of  
324 frequency power at fronto-central electrodes with context (short vs long) and prior interval as  
325 predictors for every time-frequency point during the overlapping interval. Figure 5A shows the slope  
326 values representing the effect of context on the power of the different frequencies over time. We  
327 found a positive cluster in the window 0.48-0.84 s after interval onset in the 23-30 Hz frequency range  
328 ( $p = .045$ ), indicating increased beta power in the long context compared to the short context (see the  
329 outlined area in Figure 5A). This beta effect is further illustrated in Figure 3C, which shows the  
330 average power in the 23-30 Hz over time, for the overlapping interval in the short and long context.  
331 Figure 5B shows the slope values for prior interval, for which the permutation test indicated no  
332 evidence for a cluster of slopes different from zero ( $ps > .051$ ). In summary, these results suggest that  
333 fronto-central beta power was higher in the long compared to the short context, while there was no  
334 evidence for a similar influence of the previous trial.

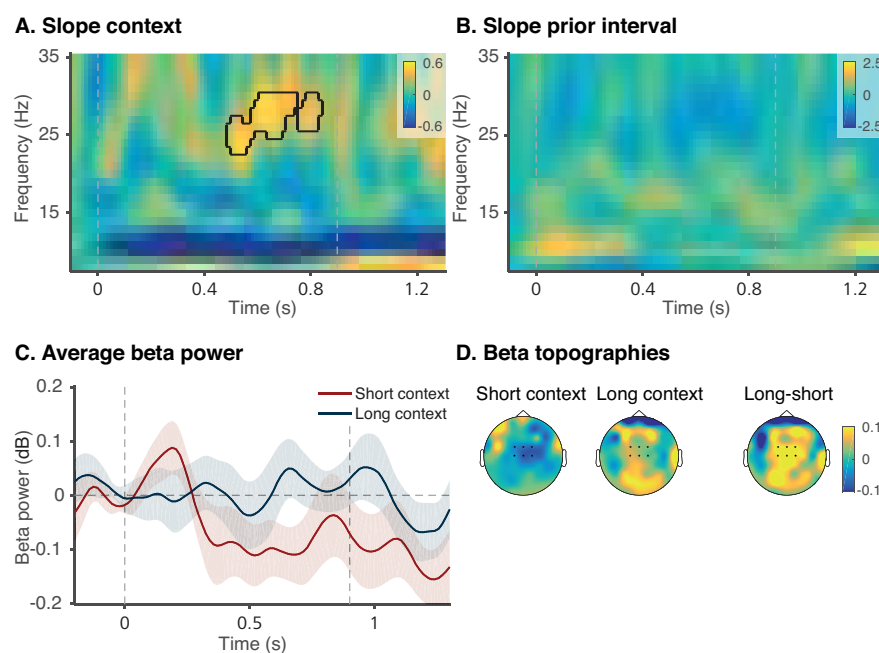


**Figure 5.** Slope values of regression on frequency power at fronto-central electrode cluster (electrodes Cz, C1, C2, FCz, FC1, FC2) relative to the onset of the perception phase. A) Slope values of the factor Context (short vs long) in the regression analysis at every time-frequency point. The outlined area marks a significant cluster according to the cluster-based permutation test performed in the time window 0-1.2 s and the frequency window 8-30 Hz. B) Slope values of the factor prior interval in the regression analysis predicting power. There was no evidence for significant clusters. In both panels, vertical dashed grey lines indicate the onset and offset of the perception phase. C) Average beta power in the time and frequency range of the significant cluster (23-30 Hz) for the short and long context for the overlapping interval. Error shading represents represent the standard error of the mean. D) Topographies of beta power for the overlapping interval, in the time and frequency range of the significant cluster, for the short context, the long context, and their difference.

### 335 **Linking EEG signatures and behavior**

336 Figure 1C shows the effect of single-trial EEG signatures on reproductions of the overlapping  
337 interval. For illustration purposes, the single-trial EEG amplitudes and latencies were divided into  
338 tertiles (low/short, medium, high/long) for each participant and context, and the average reproduction  
339 was plotted for each tertile. The LMMs showed no evidence that single-trial CNV and beta power in  
340 the perception phase predicted reproductions in the reproduction phase ( $\beta = 0.0003$ ,  $SE = 0.0004$ ,  $t =$   
341  $0.85$ ,  $p = .395$  and  $\beta = 0.0003$ ,  $SE = 0.0019$ ,  $t = -0.51$ ,  $p = .614$ , respectively). This was also the case  
342 for P2 latency, with a trend towards shorter reproductions for later P2 peaks ( $\beta = -0.08$ ,  $SE = 0.04$ ,  $t =$   
343  $-1.80$ ,  $p = .072$ ). However, P2 amplitude after perception phase offset was predictive of that trial's  
344 reproduction ( $\beta = -0.0010$ ,  $SE = 0.0003$ ,  $t = -3.45$ ,  $p < .001$ ). As the  $\beta$ -value indicates, higher P2 peaks  
345 were followed by shorter reproductions. Given that context, interval and prior interval were also  
346 included as fixed factors in the LMM, these results cannot be attributed to a mediating influence of  
347 context, and therefore suggest that trial-by-trial variation in P2 amplitude might be a reliable predictor  
348 of reproductions.

349 We additionally tested whether participants with a large behavioral context effect for the  
350 overlapping interval also showed a large context effect in the EEG signatures. This between-  
351 participant relationship between these measures is depicted in Figure 1D. Analysis showed that the  
352 individual behavioral context effect was correlated with the P2 amplitude difference between contexts  
353 ( $r(23) = -.37$ ,  $p = .033$ ). We found no evidence for a similar relationship with P2 latency ( $r(23) = -.18$ ,  
354  $p = .196$ ), CNV amplitude ( $r(23) = .19$ ,  $p = .180$ ) or beta power ( $r(23) = -.22$ ,  $p = .861$ ). Thus, in line  
355 with the single trial analysis, P2 amplitude differences predict reproduction outcomes.

### 356 **Discussion**

357 As the temporal locus of Bayesian computations in human time estimation is still unknown,  
358 we investigated whether temporal context actively influences neural signatures during the perception  
359 of time intervals. Behaviorally, we found that reproductions were biased towards the global temporal  
360 context as well as the duration in the previous trial. EEG results showed that CNV, P2 and beta power  
361 were modulated by previously perceived intervals, and that context could be decoded from transient

362 brain dynamics at an early stage during perception. These results indicate that previously perceived  
363 durations actively affect EEG signatures during interval estimation, showing that prior experiences act  
364 directly on perception. This observation goes against the (implicit) assumption of time perception  
365 models that the likelihood is weighted with the prior only after perception. It is, however, in line with  
366 recent behavioral evidence showing that context asserts its influence at early sensory stages (Cicchini  
367 et al., 2020; Zimmermann & Cicchini, 2020). Our findings suggest that experiences with the global  
368 and recent temporal context actively calibrate cortical dynamics, in which the CNV and beta power  
369 may reflect the anticipation of stimulus duration, and the P2 component the active evaluation of the  
370 interval in the current context. Crucially, by focusing on the perception phase in a reproduction  
371 paradigm, this is the first work demonstrating context effects that are not linked to explicit motor  
372 preparation or response decisions.

373         Our findings argue against the idea that the CNV reflects the neural counterpart of the  
374 absolute accumulator in pacemaker-accumulator models (Casini & Vidal, 2011; Macar & Besson,  
375 1985; Macar & Vidal, 2004; Macar, Vidal, & Casini, 1999; Macar & Vitton, 1982; Pfeuty, Ragot, &  
376 Pouthas, 2005), since no differences based on prior experience would be expected during the  
377 perception of an interval. Instead, we found that the CNV during the perception of the overlapping  
378 interval was more negative for the short compared to the long context, and for shorter previous  
379 durations. This is consistent with anticipation and preparation accounts of the CNV (e.g., Boehm et  
380 al., 2014; Elbert, 1993; Leuthold, Sommer, & Ulrich, 2004; Mento, 2013; Ng et al., 2011; Scheibe,  
381 Schubert, Sommer, & Heekeren, 2009) and pacemaker-accumulator models that propose adaptive  
382 spike rate accumulation (Simen, Balci, deSouza, Cohen, & Holmes, 2011): When interval offset is  
383 expected quickly after onset, CNV amplitude increases more rapidly. This adaptation is in line with  
384 studies showing a faster CNV development for relatively short foreperiods (Miniussi, Wilding, Coull,  
385 & Nobre, 1999; Müller-Gethmann, Ulrich, & Rinkenauer, 2003; Trillenber, Verleger, Wascher,  
386 Wauschkuhn, & Wessel, 2000; Van der Lubbe, Los, Jaśkowski, & Verleger, 2004), shorter standard  
387 durations in an interval comparison task (Pfeuty et al., 2005), and after adaptation to a shorter interval  
388 (Li, Chen, Xiao, Liu, & Huang, 2017). The contextual adjustment of the speed with which the CNV  
389 develops suggests that neural populations in the supplementary motor area (SMA), which is typically

390 associated with the CNV (e.g., Coull, Vidal, & Burle, 2016), can perform flexible temporal scaling  
391 based on the temporal context (Remington, Egger, Narain, Wang, & Jazayeri, 2018; Remington,  
392 Narain, Hosseini, & Jazayeri, 2018; Sohn et al., 2019), even in the absence of explicit motor  
393 preparation. The prior might calibrate the speed of neural dynamics through different initial states at  
394 the onset of the perception phase (Remington, Egger, et al., 2018; Sohn et al., 2019), as our  
395 multivariate pattern analysis showed that global context can be decoded from EEG dynamics  
396 immediately after the onset of the perception phase. Although the precise onset of significant  
397 decoding should be interpreted with caution since the moving window approach and low-pass filtering  
398 could smear out the accuracy over time (Grootswagers, Wardle, & Carlson, 2017), these results  
399 suggest that temporal context affects the instantaneous neural response to to-be-timed stimuli.

400         The active anticipation based on context was also indexed by the P2 component. Specifically,  
401 P2 amplitude increased with longer current durations, suggesting that it reflects hazard-based  
402 expectancy: the probability that the interval offset will occur, given that it has not yet occurred  
403 (Nobre, Correa, & Coull, 2007). This is in line with previous studies showing that longer ISIs increase  
404 P2 amplitude (e.g., Pereira et al., 2014; Röder et al., 2000). Importantly, however, P2 amplitude  
405 decreased with longer previous durations, showing that the expectations are updated to the current  
406 temporal context, even on a trial-by-trial basis. These results complement previous studies showing  
407 that temporal expectancy modulates ERP amplitude (e.g., Kononowicz & van Rijn, 2014; Li et al.,  
408 2017; Todorovic & de Lange, 2012; Todorovic, van Ede, Maris, & de Lange, 2011; Wacongne et al.,  
409 2011). Interestingly, P2 amplitude at perception phase offset predicted interval reproductions, and  
410 participants' behavioral context effect correlated with their context-based P2 effect. The lack of an  
411 equivalent CNV-effect highlights the predictive quality of the P2 (Kononowicz & van Rijn, 2014;  
412 Kruijne et al., 2021), and indicates that the neural state at the end of the perception phase sets the  
413 speed of cortical dynamics during reproduction (Sohn et al., 2019). Global context additionally  
414 influenced beta power, such that beta power was higher in the long compared to the short context, in  
415 line with effects of beta power in single trial analyses (Kononowicz & van Rijn, 2015). Although beta  
416 power has been proposed to reflect motor inhibition (Alegre et al., 2004; Hwang, Ghuman, Manoach,  
417 Jones, & Luna, 2014; Kononowicz & van Rijn, 2015; Kühn et al., 2004), and most studies on the link

418 between beta power and timing have a strong motor component, our results suggest that synchronized  
419 beta oscillations also play a role during interval perception after which no immediate motor response  
420 is required. This finding complements recent studies showing that the accuracy and precision of time  
421 estimates depend on beta (Wiener et al., 2018) and alpha-beta coupling (Kononowicz, Sander, van  
422 Rijn, & Van Wassenhove, 2020). Additionally, the current global context effect on beta is in line with  
423 Wiener et al.'s finding that longer previous durations increased beta power in the current trial. It has  
424 to be noted, however, that we found no evidence for similar sequential effects on beta.

425         Besides the auditory stimuli which participants had to time, the current paradigm also  
426 consisted of visual stimuli that indicated the phase of the trial (i.e., perception or reproduction). The  
427 general overestimation we found in the behavioral results might potentially be explained by the  
428 integration of these visual stimuli in temporal estimation (Shi & Burr, 2016). Future studies might  
429 look further into potential modality differences in contextual calibration and their neural  
430 underpinnings (Rhodes, Seth, & Roseboom, 2018; Roach et al., 2017; Zimmermann & Cicchini,  
431 2020). Furthermore, we found no significant decoding corresponding to the windows of CNV  
432 differences. This can be explained by the specific decoding method we employed, which focused on  
433 transient dynamics, filtering out the stable CNV activity by baselining within a moving window. In  
434 addition, decoding might be especially sensitive to stimulus onset and offset, with accuracy peaking  
435 shortly afterwards and slowly dropping as the neural synchronization declines (e.g., Wolff et al.,  
436 2017, 2020).

437         A comparison to Wiener and Thompson (2015), who found a larger CNV amplitude for  
438 *longer* prior durations, suggests that contextual ERP effects might be dependent on the specific  
439 experimental paradigm. In contrast to our reproduction experiment, their bisection task requires an  
440 active decision during perception, and the CNV has been shown to reflect this decision process by  
441 deflecting or plateauing after the standard interval in memory has been reached (Macar & Vidal,  
442 2004; Ng et al., 2011; Pfeuty, Ragot, & Pouthas, 2003). A similar explanation could account for the  
443 different nature of our offset P2 effect compared to Kononowicz and van Rijn (2014), who found a V-  
444 shaped P2 amplitude attenuation in a temporal comparison task (but see Kruijne et al., 2021). This  
445 pattern reflects active comparison to the standard interval, which is not applicable to the current

446 reproduction paradigm. In addition, the P2 measured in the current study shows similarities to the  
447 positive offset peak named the late positive component of timing (LPCt) (Gontier et al., 2009; Paul et  
448 al., 2011; Wiener & Thompson, 2015), although it has been argued that the P2 reflects perceptual  
449 predictive processes while the LPCt indexes decision making (Kononowicz, van Rijn, & Meck, 2016).  
450 The extent to which these components indeed reflect similar processes is still an open question, and  
451 their occurrence seems to depend on the specific nature of the task. Future studies might directly  
452 compare these neural differences in paradigms involving decision, motor or only perceptual timing  
453 requirements.

454         In conclusion, our results show that previous durations actively influence flexible neural  
455 dynamics during temporal encoding. These findings indicate that previous experiences in memory  
456 create expectations that in turn calibrate our perception of the environment. The adaptive influence of  
457 prior knowledge on perception could represent a more general Bayesian mechanism of magnitude  
458 estimation (Petzschner, Glasauer, & Stephan, 2015), falsifying a class of models that assume discrete,  
459 post-perceptual stages in which previous experiences exert their influence.

460  
461  
462  
463  
464  
465  
466  
467  
468  
469  
470

### **Acknowledgements**

This research has been partially supported by the EU Horizon 2020 FET Proactive grant TIMESTORM - Mind and Time: Investigation of the Temporal Traits of Human-Machine Convergence (Grant number 641100) and by the research programme Interval Timing in the Real World financed by the Netherlands Organisation for Scientific Research (NWO, Grant number 453-16-005, awarded to Hedderik van Rijn). The funding agencies had no involvement in the design of the study, the analysis of the data, writing of the report, or in the decision to submit the article for publication. We thank Sarah Maaß for fruitful discussions and programming the experiment, Ronja Eike for her help in data collection and preprocessing, Emil Uffelmann for his help in data collection, and Michael Wolff and Güven Kandemir for sharing their decoding knowledge with us.

471

## References

- 472 Acerbi, L., Wolpert, D. M., & Vijayakumar, S. (2012). Internal Representations of Temporal Statistics  
473 and Feedback Calibrate Motor-Sensory Interval Timing. *PLoS Computational Biology*, 8(11).  
474 <https://doi.org/10.1371/journal.pcbi.1002771>
- 475 Alegre, M., De Gurtubay, I. G., Labarga, A., Iriarte, J., Malanda, A., & Artieda, J. (2004). Alpha and  
476 beta oscillatory activity during a sequence of two movements. *Clinical Neurophysiology*, 115(1),  
477 124–130. [https://doi.org/10.1016/S1388-2457\(03\)00311-0](https://doi.org/10.1016/S1388-2457(03)00311-0)
- 478 Bates, D., Mächler, M., Bolker, B. M., & Walker, S. C. (2015). Fitting linear mixed-effects models  
479 using lme4. *Journal of Statistical Software*, 67(1). <https://doi.org/10.18637/jss.v067.i01>
- 480 Boehm, U., Van Maanen, L., Forstmann, B., & van Rijn, H. (2014). Trial-by-trial fluctuations in CNV  
481 amplitude reflect anticipatory adjustment of response caution. *NeuroImage*, 96, 95–105.  
482 <https://doi.org/10.1016/j.neuroimage.2014.03.063>
- 483 Brainard, D. H. (1997). The Psychophysics Toolbox. *Spatial Vision*, 10(4), 433–436.  
484 <https://doi.org/10.1163/156856897X00357>
- 485 Casini, L., & Vidal, F. (2011). The SMAs: Neural substrate of the temporal accumulator? *Frontiers in*  
486 *Integrative Neuroscience*, 5, 1–3. <https://doi.org/10.3389/fnint.2011.00035>
- 487 Cicchini, G. M., Arrighi, R., Cecchetti, L., Giusti, M., & Burr, D. C. (2012). Optimal encoding of  
488 interval timing in expert percussionists. *Journal of Neuroscience*, 32(3), 1056–1060.  
489 <https://doi.org/10.1523/JNEUROSCI.3411-11.2012>
- 490 Cicchini, G. M., Benedetto, A., & Burr, D. C. (2020). Perceptual history propagates down to early  
491 levels of sensory analysis. *Current Biology*. <https://doi.org/10.1016/j.cub.2020.12.004>
- 492 Cicchini, G. M., Mikellidou, K., & Burr, D. (2017). Serial dependencies act directly on perception.  
493 *Journal of Vision*, 17(14). <https://doi.org/10.1167/17.14.6>
- 494 Coull, J. T., Vidal, F., & Burle, B. (2016). When to act, or not to act: That's the SMA's question.  
495 *Current Opinion in Behavioral Sciences*, Vol. 8, pp. 14–21.  
496 <https://doi.org/10.1016/j.cobeha.2016.01.003>
- 497 De Maesschalck, R., Jouan-Rimbaud, D., & Massart, D. L. (2000). The Mahalanobis distance.  
498 *Chemometrics and Intelligent Laboratory Systems*, 50(1), 1–18. [https://doi.org/10.1016/S0169-](https://doi.org/10.1016/S0169-7439(99)00047-7)  
499 [7439\(99\)00047-7](https://doi.org/10.1016/S0169-7439(99)00047-7)
- 500 Di Luca, M., & Rhodes, D. (2016). Optimal Perceived Timing: Integrating Sensory Information with  
501 Dynamically Updated Expectations. *Scientific Reports*, 6, 1–15.  
502 <https://doi.org/10.1038/srep28563>
- 503 Dyjas, O., Bausenhardt, K. M., & Ulrich, R. (2012). Trial-by-trial updating of an internal reference in  
504 discrimination tasks: Evidence from effects of stimulus order and trial sequence. *Attention,*  
505 *Perception, and Psychophysics*, 74(8), 1819–1841. <https://doi.org/10.3758/s13414-012-0362-4>
- 506 Elbert, T. (1993). Slow Cortical Potentials Reflect the Regulation of Cortical Excitability. In *Slow*  
507 *Potential Changes in the Human Brain* (pp. 235–251). [https://doi.org/10.1007/978-1-4899-1597-](https://doi.org/10.1007/978-1-4899-1597-9_15)  
508 [9\\_15](https://doi.org/10.1007/978-1-4899-1597-9_15)
- 509 Gontier, E., Paul, I., Le Dantec, C., Pouthas, V., Jean-Marie, G., Bernard, C., ... Rebaï, M. (2009).  
510 ERPs in Anterior and Posterior Regions Associated With Duration and Size Discriminations.  
511 *Neuropsychology*, 23(5), 668–678. <https://doi.org/10.1037/a0015757>
- 512 Grootswagers, T., Wardle, S. G., & Carlson, T. A. (2017). Decoding dynamic brain patterns from  
513 evoked responses: A tutorial on multivariate pattern analysis applied to time series neuroimaging  
514 data. *Journal of Cognitive Neuroscience*, 29(4), 677–697. [https://doi.org/10.1162/jocn\\_a\\_01068](https://doi.org/10.1162/jocn_a_01068)
- 515 Gu, B. M., Jurkowski, A. J., Lake, J. I., Malapani, C., & Meck, W. H. (2015). Bayesian Models of



- 516 Interval Timing and Distortions in Temporal Memory as a Function of Parkinson’s Disease and  
517 Dopamine-Related Error Processing. In *Time Distortions in Mind* (pp. 281–327).  
518 [https://doi.org/10.1163/9789004230699\\_012](https://doi.org/10.1163/9789004230699_012)
- 519 Haegens, S., Nacher, V., Hernández, A., Luna, R., Jensen, O., & Romo, R. (2011). Beta oscillations in  
520 the monkey sensorimotor network reflect somatosensory decision making. *Proceedings of the*  
521 *National Academy of Sciences of the United States of America*, *108*(26), 10708–10713.  
522 <https://doi.org/10.1073/pnas.1107297108>
- 523 Hallez, Q., Damsma, A., Rhodes, D., van Rijn, H., & Droit-Volet, S. (2019). The dynamic effect of  
524 context on interval timing in children and adults. *Acta Psychologica*, *192*, 87–93.  
525 <https://doi.org/10.1016/j.actpsy.2018.10.004>
- 526 Hwang, K., Ghuman, A. S., Manoach, D. S., Jones, S. R., & Luna, B. (2014). Cortical neurodynamics  
527 of inhibitory control. *Journal of Neuroscience*, *34*(29), 9551–9561.  
528 <https://doi.org/10.1523/JNEUROSCI.4889-13.2014>
- 529 Jazayeri, M., & Shadlen, M. N. (2010). Temporal context calibrates interval timing. *Nature*  
530 *Neuroscience*, *13*(8), 1020–1026. <https://doi.org/10.1038/nn.2590>
- 531 Jenkinson, N., & Brown, P. (2011). New insights into the relationship between dopamine, beta  
532 oscillations and motor function. *Trends in Neurosciences*, *34*(12), 611–618.  
533 <https://doi.org/10.1016/j.tins.2011.09.003>
- 534 Kleiner, M., Brainard, D. H., Pelli, D. G., Broussard, C., Wolf, T., & Niehorster, D. (2007). What’s  
535 new in Psychtoolbox-3? *Perception*, *36*, S14. <https://doi.org/10.1068/v070821>
- 536 Kononowicz, T. W., Sander, T., Van Rijn, H., & Van Wassenhove, V. (2020). Precision timing with  
537  $\alpha$ - $\beta$  oscillatory coupling: Stopwatch or motor control? *Journal of Cognitive Neuroscience*,  
538 *32*(9), 1624–1636. [https://doi.org/10.1162/jocn\\_a\\_01570](https://doi.org/10.1162/jocn_a_01570)
- 539 Kononowicz, T. W., & van Rijn, H. (2014). Decoupling interval timing and climbing neural activity:  
540 A dissociation between CNV and N1P2 amplitudes. *Journal of Neuroscience*, *34*(8), 2931–2939.  
541 <https://doi.org/10.1523/JNEUROSCI.2523-13.2014>
- 542 Kononowicz, T. W., & van Rijn, H. (2015). Single trial beta oscillations index time estimation.  
543 *Neuropsychologia*, *75*, 381–389. <https://doi.org/10.1016/j.neuropsychologia.2015.06.014>
- 544 Kononowicz, T. W., van Rijn, H., & Meck, W. H. (2016). Timing and time perception: a critical  
545 review of neural timing signatures before, during, and after the To-Be-Timed Interval. In *Stevens*  
546 *Handbook of Experimental Psychology and Cognitive Neuroscience (4th ed.)*.
- 547 Kruijne, W., Olivers, C. N. L., & van Rijn, H. (2021). Neural repetition suppression modulates time  
548 perception: Evidence from electrophysiology and pupillometry. *BioRxiv*, 2020.07.31.230508.  
549 <https://doi.org/10.1101/2020.07.31.230508>
- 550 Kühn, A. A., Williams, D., Kupsch, A., Limousin, P., Hariz, M., Schneider, G. H., ... Brown, P.  
551 (2004). Event-related beta desynchronization in human subthalamic nucleus correlates with  
552 motor performance. *Brain*, *127*(4), 735–746. <https://doi.org/10.1093/brain/awh106>
- 553 Ledoit, O., & Wolf, M. (2004). Honey, I shrunk the sample covariance matrix. *Journal of Portfolio*  
554 *Management*, *30*(4), 110–119. <https://doi.org/10.3905/jpm.2004.110>
- 555 Lemm, S., Blankertz, B., Dickhaus, T., & Müller, K. R. (2011). Introduction to machine learning for  
556 brain imaging. *NeuroImage*, *56*(2), 387–399. <https://doi.org/10.1016/j.neuroimage.2010.11.004>
- 557 Leuthold, H., Sommer, W., & Ulrich, R. (2004). Preparing for action: Inferences from CNV and LRP.  
558 *Journal of Psychophysiology*, *18*(2–3), 77–88. <https://doi.org/10.1027/0269-8803.18.23.77>
- 559 Li, B., Chen, Y., Xiao, L., Liu, P., & Huang, X. (2017). Duration adaptation modulates EEG  
560 correlates of subsequent temporal encoding. *NeuroImage*, *147*(2), 143–151.  
561 <https://doi.org/10.1016/j.neuroimage.2016.12.015>

- 562 Liesefeld, H. R. (2018). Estimating the Timing of Cognitive Operations With MEG/EEG Latency  
563 Measures: A Primer, a Brief Tutorial, and an Implementation of Various Methods. *Frontiers in*  
564 *Neuroscience*, *12*. <https://doi.org/10.3389/fnins.2018.00765>
- 565 Luck, S. J. (2005). An Introduction to Event-Related Potentials and Their Neural Origins. *An*  
566 *Introduction to the Event-Related Potential Technique*.
- 567 Maaß, S. C., Riemer, M., Wolbers, T., & van Rijn, H. (2019). Timing deficiencies in amnesic Mild  
568 Cognitive Impairment: Disentangling clock and memory processes. *Behavioural Brain*  
569 *Research*, *373*, 112110. <https://doi.org/10.1016/j.bbr.2019.112110>
- 570 Maaß, S. C., Schlichting, N., & van Rijn, H. (2019). Eliciting contextual temporal calibration: The  
571 effect of bottom-up and top-down information in reproduction tasks. *Acta Psychologica*, *199*,  
572 102898. <https://doi.org/10.1016/j.actpsy.2019.102898>
- 573 Macar, F., & Besson, M. (1985). Contingent negative variation in processes of expectancy, motor  
574 preparation and time estimation. *Biological Psychology*, *21*(4), 293–307.  
575 [https://doi.org/10.1016/0301-0511\(85\)90184-X](https://doi.org/10.1016/0301-0511(85)90184-X)
- 576 Macar, F., & Vidal, F. (2004). Event-related potentials as indices of time processing: A review.  
577 *Journal of Psychophysiology*, Vol. 18, pp. 89–104. <https://doi.org/10.1027/0269-8803.18.23.89>
- 578 Macar, F., Vidal, F., & Casini, L. (1999). The supplementary motor area in motor and sensory timing:  
579 Evidence from slow brain potential changes. *Experimental Brain Research*, *125*(3), 271–280.  
580 <https://doi.org/10.1007/s002210050683>
- 581 Macar, F., & Vitton, N. (1982). An early resolution of contingent negative variation (CNV) in time  
582 discrimination. *Electroencephalography and Clinical Neurophysiology*, *54*(4), 426–435.  
583 [https://doi.org/10.1016/0013-4694\(82\)90206-1](https://doi.org/10.1016/0013-4694(82)90206-1)
- 584 Maris, E., & Oostenveld, R. (2007). Nonparametric statistical testing of EEG- and MEG-data. *Journal*  
585 *of Neuroscience Methods*, *164*(1), 177–190. <https://doi.org/10.1016/j.jneumeth.2007.03.024>
- 586 Mento, G. (2013). The passive CNV: Carving out the contribution of task-related processes to  
587 expectancy. *Frontiers in Human Neuroscience*, *7*, 827.  
588 <https://doi.org/10.3389/fnhum.2013.00827>
- 589 Miniussi, C., Wilding, E. L., Coull, J. T., & Nobre, A. C. (1999). Orienting attention in time.  
590 Modulation of brain potentials. *Brain*, *122*(8), 1507–1518.  
591 <https://doi.org/10.1093/brain/122.8.1507>
- 592 Müller-Gethmann, H., Ulrich, R., & Rinkenauer, G. (2003). Locus of the effect of temporal  
593 preparation: Evidence from the lateralized readiness potential. *Psychophysiology*, *40*(4), 597–  
594 611. <https://doi.org/10.1111/1469-8986.00061>
- 595 Ng, K. K., Tobin, S., & Penney, T. B. (2011). Temporal accumulation and decision processes in the  
596 duration bisection task revealed by contingent negative variation. *Frontiers in Integrative*  
597 *Neuroscience*, *5*, 77. <https://doi.org/10.3389/fnint.2011.00077>
- 598 Nobre, A. C., Correa, A., & Coull, J. (2007). The hazards of time. *Current Opinion in Neurobiology*,  
599 *17*(4), 465–470. <https://doi.org/10.1016/j.conb.2007.07.006>
- 600 Oostenveld, R., Fries, P., Maris, E., & Schoffelen, J. M. (2011). FieldTrip: Open source software for  
601 advanced analysis of MEG, EEG, and invasive electrophysiological data. *Computational*  
602 *Intelligence and Neuroscience*, *2011*. <https://doi.org/10.1155/2011/156869>
- 603 Paul, I., Wearden, J., Bannier, D., Gontier, E., Le Dantec, C., & Rebaï, M. (2011). Making decisions  
604 about time: Event-related potentials and judgements about the equality of durations. *Biological*  
605 *Psychology*, *88*(1), 94–103. <https://doi.org/10.1016/j.biopsycho.2011.06.013>
- 606 Pereira, D. R., Cardoso, S., Ferreira-Santos, F., Fernandes, C., Cunha-Reis, C., Paiva, T. O., ...  
607 Marques-Teixeira, J. (2014). Effects of inter-stimulus interval (ISI) duration on the N1 and P2

- 608 components of the auditory event-related potential. *International Journal of Psychophysiology*,  
609 94(3), 311–318. <https://doi.org/10.1016/j.ijpsycho.2014.09.012>
- 610 Petzschner, F. H., Glasauer, S., & Stephan, K. E. (2015). A Bayesian perspective on magnitude  
611 estimation. *Trends in Cognitive Sciences*, 19(5), 285–293.  
612 <https://doi.org/10.1016/j.tics.2015.03.002>
- 613 Pfeuty, M., Ragot, R., & Pouthas, V. (2003). When time is up: CNV time course differentiates the  
614 roles of the hemispheres in the discrimination of short tone durations. *Experimental Brain*  
615 *Research*, 151(3), 372–379. <https://doi.org/10.1007/s00221-003-1505-6>
- 616 Pfeuty, M., Ragot, R., & Pouthas, V. (2005). Relationship between CNV and timing of an upcoming  
617 event. *Neuroscience Letters*, 382(1–2), 106–111. <https://doi.org/10.1016/j.neulet.2005.02.067>
- 618 R Core Development Team. (2013). A language and environment for statistical computing. *R*  
619 *Foundation for Statistical Computing*, Vol. 1. Retrieved from <http://www.r-project.org/>
- 620 Remington, E. D., Egger, S. W., Narain, D., Wang, J., & Jazayeri, M. (2018). A Dynamical Systems  
621 Perspective on Flexible Motor Timing. *Trends in Cognitive Sciences*, 22(10), 938–952.  
622 <https://doi.org/10.1016/j.tics.2018.07.010>
- 623 Remington, E. D., Narain, D., Hosseini, E. A., & Jazayeri, M. (2018). Flexible Sensorimotor  
624 Computations through Rapid Reconfiguration of Cortical Dynamics. *Neuron*, 98(5), 1005-  
625 1019.e5. <https://doi.org/10.1016/j.neuron.2018.05.020>
- 626 Rhodes, D., Seth, A. K., & Roseboom, W. (2018). Multiple Duration Priors Within and Across the  
627 Senses. *BioRxiv*, 467027. <https://doi.org/10.1101/467027>
- 628 Roach, N. W., McGraw, P. V., Whitaker, D. J., & Heron, J. (2017). Generalization of prior  
629 information for rapid Bayesian time estimation. *Proceedings of the National Academy of*  
630 *Sciences of the United States of America*, 114(2), 412–417.  
631 <https://doi.org/10.1073/pnas.1610706114>
- 632 Röder, B., Rösler, F., & Neville, H. J. (2000). Event-related potentials during auditory language  
633 processing in congenitally blind and sighted people. *Neuropsychologia*, 38(11), 1482–1502.  
634 [https://doi.org/10.1016/S0028-3932\(00\)00057-9](https://doi.org/10.1016/S0028-3932(00)00057-9)
- 635 Scheibe, C., Schubert, R., Sommer, W., & Heekeren, H. R. (2009). Electrophysiological evidence for  
636 the effect of prior probability on response preparation. *Psychophysiology*, 46(4), 758–770.  
637 <https://doi.org/10.1111/j.1469-8986.2009.00825.x>
- 638 Schlichting, N., Damsma, A., Aksoy, E. E., Wächter, M., Asfour, T., & van Rijn, H. (2018). Temporal  
639 Context Influences the Perceived Duration of Everyday Actions: Assessing the Ecological  
640 Validity of Lab-Based Timing Phenomena. *Journal of Cognition*, 2(1).  
641 <https://doi.org/10.5334/joc.4>
- 642 Shi, Z., & Burr, D. (2016). Predictive coding of multisensory timing. *Current Opinion in Behavioral*  
643 *Sciences*, 8, 200–206. <https://doi.org/10.1016/j.cobeha.2016.02.014>
- 644 Shi, Z., Church, R. M., & Meck, W. H. (2013). Bayesian optimization of time perception. *Trends in*  
645 *Cognitive Sciences*, 17(11), 556–564. <https://doi.org/10.1016/j.tics.2013.09.009>
- 646 Simen, P., Balci, F., deSouza, L., Cohen, J. D., & Holmes, P. (2011). A model of interval timing by  
647 neural integration. *Journal of Neuroscience*, 31(25), 9238–9253.  
648 <https://doi.org/10.1523/JNEUROSCI.3121-10.2011>
- 649 Sohn, H., Narain, D., Meirhaeghe, N., & Jazayeri, M. (2019). Bayesian Computation through Cortical  
650 Latent Dynamics. *Neuron*, 103(5), 934–947.e5. <https://doi.org/10.1016/j.neuron.2019.06.012>
- 651 St. John-Saaltink, E., Kok, P., Lau, H. C., & De Lange, F. P. (2016). Serial dependence in perceptual  
652 decisions is reflected in activity patterns in primary visual cortex. *Journal of Neuroscience*,  
653 36(23), 6186–6192. <https://doi.org/10.1523/JNEUROSCI.4390-15.2016>

- 654 Taatgen, N. A., & van Rijn, H. (2011). Traces of times past: Representations of temporal intervals in  
655 memory. *Memory and Cognition*, 39(8), 1546–1560. <https://doi.org/10.3758/s13421-011-0113-0>
- 656 Tanner, D., Morgan-Short, K., & Luck, S. J. (2015). How inappropriate high-pass filters can produce  
657 artifactual effects and incorrect conclusions in ERP studies of language and cognition.  
658 *Psychophysiology*, 52(8), 997–1009. <https://doi.org/10.1111/psyp.12437>
- 659 Todorovic, A., & de Lange, F. P. (2012). Repetition suppression and expectation suppression are  
660 dissociable in time in early auditory evoked fields. *Journal of Neuroscience*, 32(39), 13389–  
661 13395. <https://doi.org/10.1523/JNEUROSCI.2227-12.2012>
- 662 Todorovic, A., van Ede, F., Maris, E., & de Lange, F. P. (2011). Prior expectation mediates neural  
663 adaptation to repeated sounds in the auditory cortex: An MEG study. *Journal of Neuroscience*,  
664 31(25), 9118–9123. <https://doi.org/10.1523/JNEUROSCI.1425-11.2011>
- 665 Trillenber, P., Verleger, R., Wascher, E., Wauschkuhn, B., & Wessel, K. (2000). CNV and temporal  
666 uncertainty with “ageing” and “non-ageing” S1-S2 intervals. *Clinical Neurophysiology*, 111(7),  
667 1216–1226. [https://doi.org/10.1016/S1388-2457\(00\)00274-1](https://doi.org/10.1016/S1388-2457(00)00274-1)
- 668 Van der Lubbe, R. H. J., Los, S. A., Jaśkowski, P., & Verleger, R. (2004). Being prepared on time: On  
669 the importance of the previous foreperiod to current preparation, as reflected in speed, force and  
670 preparation-related brain potentials. *Acta Psychologica*, 116(3), 245–262.  
671 <https://doi.org/10.1016/j.actpsy.2004.03.003>
- 672 Wacongne, C., Labyt, E., Van Wassenhove, V., Bekinschtein, T., Naccache, L., & Dehaene, S.  
673 (2011). Evidence for a hierarchy of predictions and prediction errors in human cortex.  
674 *Proceedings of the National Academy of Sciences of the United States of America*, 108(51),  
675 20754–20759. <https://doi.org/10.1073/pnas.1117807108>
- 676 Wiener, M., Parikh, A., Krakow, A., & Coslett, H. B. (2018). An intrinsic role of beta oscillations in  
677 memory for time estimation. *Scientific Reports*, 8(1), 1–17. <https://doi.org/10.1038/s41598-018-26385-6>
- 679 Wiener, M., & Thompson, J. C. (2015). Repetition enhancement and memory effects for duration.  
680 *NeuroImage*, 113, 268–278. <https://doi.org/10.1016/j.neuroimage.2015.03.054>
- 681 Wiener, M., Thompson, J. C., & Branch Coslett, H. (2014). Continuous carryover of temporal context  
682 dissociates response bias from perceptual influence for duration. *PLoS ONE*, 9(6).  
683 <https://doi.org/10.1371/journal.pone.0100803>
- 684 Wolff, M. J., Jochim, J., Akyürek, E. G., & Stokes, M. G. (2017). Dynamic hidden states underlying  
685 working-memory-guided behavior. *Nature Neuroscience*, 20(6), 864–871.  
686 <https://doi.org/10.1038/nn.4546>
- 687 Wolff, M. J., Kandemir, G., Stokes, M. G., & Akyürek, E. G. (2020). Unimodal and Bimodal Access  
688 to Sensory Working Memories by Auditory and Visual Impulses. *The Journal of Neuroscience* :  
689 *The Official Journal of the Society for Neuroscience*, 40(3), 671–681.  
690 <https://doi.org/10.1523/JNEUROSCI.1194-19.2019>
- 691 Zimmermann, E., & Cicchini, G. M. (2020). Temporal Context affects interval timing at the  
692 perceptual level. *Scientific Reports*. <https://doi.org/10.1038/s41598-020-65609-6>
- 693